

Beam Response Analysis for the SPring-8 Storage Ring with 4 by 4 Model Calibration Method (MCM)

H. Tanaka*, K. Soutome, M. Takao, SPring-8/JASRI, 1-1-1 Kouto, Mikazuki, Sayo, Hyogo 679-5198

J. Schimizu, The Japan Research Inst. Ltd.,
1-33-8 Shin-machi, Nishi-ku, Osaka-shi 550-0013, Japan

Abstract

Restoration of linear optics is crucial especially for third generation synchrotron radiation sources to improve key beam parameters such as emittance, momentum acceptance and so on. We have thus been analyzing the error distribution along the ring by using model calibration method (MCM) since 1998. A part of results was already utilized to improve the beam performance. The model used in MCM was recently changed from 2 by 2 to 4 by 4 formalism which can treat a complete transverse oscillation mode mixing. In this paper, we present obtained results with 4 by 4 formalism compared with those with 2 by 2 one.

1 INTRODUCTION

From the beginning of 1990, W. J. Corbett and his colleagues developed a new technique to estimate beam optics parameters via the ring model [1]. The orbit response is defined as a set of orbit differences measured by beam position monitors (BPM's) with changing strength of a certain dipole steering magnet (STM) by some amount. The different response can be obtained by using the different STM as a perturber. The idea of this method is that the realistic ring model should be obtained by fitting key parameters so that the calculated responses agree well with the corresponding measured responses. By using the model all estimated parameters are consistent with each other. Here, we do not touch the detail of parameter fitting, which one can see in Ref. [2]. This technique was successfully applied to restore the optics distortion in Advanced Light Source (ALS) [3].

We started applying 2 by 2 MCM to SPring-8 storage ring from 1998 in order to estimate the distortion of betatron functions [4]. On the other hand, top-up operation of the storage ring has recently been planned to increase the time-averaged brilliance for several bunch filling. In this case, it is essential to prevent a horizontal oscillation from coupling with a vertical one, because in-vacuum undulators limit vertical aperture to around 4 mm in half height. To optimize operational condition and control distributed linear error fields if necessary, we changed the model from 2 by 2 to 4 by 4 formalism where skew error fields and precise optics parameters for each transverse eigen mode can be estimated.

*Corresponding Author; Email: tanaka@spring8.or.jp

2 4 BY 4 RING MODEL

The ring model used here is based on linearized Hamiltonian with thin nonlinear kicks as nonlinear magnets and error fields. As a nonlinearity, we only take a sextupole magnet into account. The full transverse optics parameter calculation obeys the formalism in Ref. [5].

2.1 Energy Shift Treatment

The ring model can not treat with coupling between the transverse orbit and pathlength change. We therefore consider this effect approximately. When j -th STM at the finite linear dispersion $\eta_{z,j}$ is changed by $\theta_{z,j}$, the fractional energy shift $\Delta E_j/E$ is expressed by

$$\frac{\Delta E_j}{E} \approx \frac{\theta_{z,j} \cdot \eta_{z,j}}{\alpha \cdot L}, \quad z=x, y, \quad (1)$$

where α and L are respectively the momentum compaction factor and the circumference. The suffices x and y stand for respectively the horizontal and vertical planes. By using Eq. (1), the model response calculated by the 4 by 4 formalism, $R_{m,i,j}$ is modified as

$$R_{m,i,j} \rightarrow R_{m,i,j} + \frac{\Delta E_j}{E} \eta_{z,i}. \quad (2)$$

The suffices i and j represents respectively i -th BPM and j -th STM.

2.2 Fitting Parameters

The fitting parameters in the ring model are the following:

- Horizontal and vertical BPM gain factors $G_{x,i}$ and $G_{y,i}$ and the BPM rotation error around the beam axis q_i for 280 BPM's ($i = 1 \sim 280$).
- STM gain factors G_j and the STM rotation error around the beam axis p_j for maximum $\sim 2 \times 260$ STM's ($j = 1 \sim \text{max. } 520$).
- 236 thin integrated normal quadrupole error fields and 132 thin integrated skew quadrupole error fields.

The measured horizontal and vertical response $X_{\text{mes},i}$ and $Y_{\text{mes},i}$ are related to the model response $R_{m,i,j}$ by

$$R_{m,i,j} = \begin{bmatrix} X_{m,i,j} \\ Y_{m,i,j} \end{bmatrix} = \begin{bmatrix} \cos q_i & \sin q_i \\ -\sin q_i & \cos q_i \end{bmatrix} \begin{bmatrix} G_{x,i} X_{\text{mes},i} \\ G_{y,i} Y_{\text{mes},i} \end{bmatrix}, \quad (3)$$

where $X_{m,i,j}$ and $Y_{m,i,j}$ are respectively the horizontal and vertical model response at i -th BPM. The kick angle of j -th STM $\theta_{2,j}$ is also related to the kick angle set in the measurement through the gain factors G_j and the STM rotation error p_j .

Five normal and three skew quadrupole error fields are distributed in one Chasman Green (CG) cell and six normal and four skew quadrupole error fields are in a matching section for long straight of about 30 meter (LSS). The number of errors and their positions were optimized from the viewpoint of fitting convergence [4]. The model error field arrangement is shown in Fig. 1.

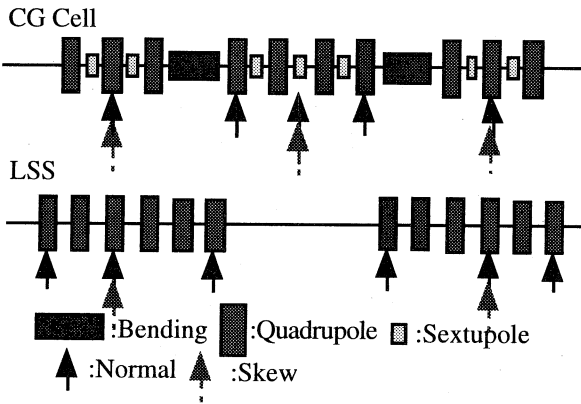


Figure 1: Arrangement of normal and skew error fields.

3 BEAM RESPONSE ANALYSIS

3.1 Beam Response Measurement

At the original operation point, cross talk between the horizontal and vertical beam responses is quite small. To enhance the cross talk, we set the operation point near by the linear differential coupling resonance line $\nu_x - \nu_y = 22$. The distance from the resonance is 0.02 ~0.03.

The step of strength change for each horizontal STM is set to 0.035 mrad and that for vertical STM is 0.05 mrad. To suppress a hysteresis effect, the direction of strength change is determined as to increase the absolute value of initial setting strength.

3.2 Fitting Convergence

The linearized sensitivities of each fitting parameter described in subsection 2.2 against beam responses are calculated with the ring model. By using the calculated sensitivity matrix, the fitting parameters are determined as to minimize the square of differences between the model and the measured responses by the least square method. Here, to solve this linear problem we used the algorithm of singular value decomposition (SVD). Since the ring model is not purely linear, the problem is iteratively solved changing the initial values of the parameters. Three iteration steps are sufficient for the good convergence.

In the SVD algorithm, the convergence also depends on the cut-off level of the eigen values. Figure 2 shows the

convergence versus cut-off level. The open squares and circles stand for respectively the s.t.d. of two normal quadrupole error distributions σ_n and that of two skew ones σ_s . Two distributions are obtained by a different sets of beam responses. The crosses stand for the r.m.s. of differences between the model and measured beam responses χ . The cut-off level V_{\min} represents the ratio against the maximum eigen value. In Fig. 2 we see that the objective χ decreases as V_{\min} decreases, but that the s.t.d. of the error distributions increases in the region where V_{\min} becomes smaller than 0.001. This shows that the convergence improvement does not contribute to the accuracy improvement of the error fields in the small cut-off region. Accordingly we set V_{\min} to 0.001 in this calculation.

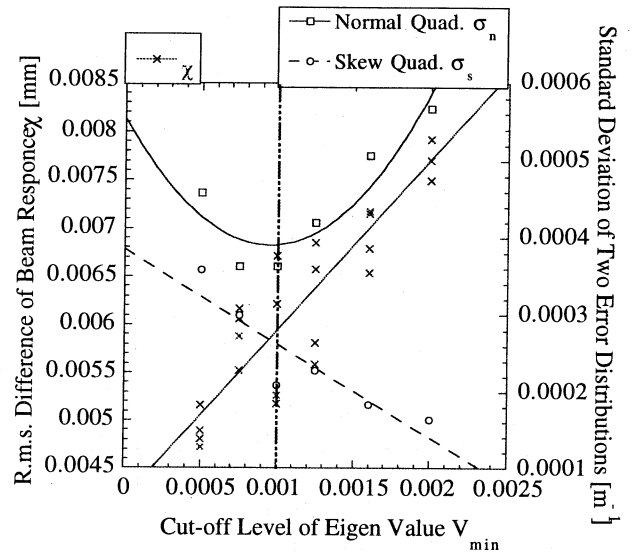


Figure 2: Fitting convergence v.s. cut-off level.

3.3 Error Field Distribution

Figure 3 shows a quarter of the estimated normal quadrupole error distributions. In the figure, the distribution calculated by 2 by 2 MCM is shown together.

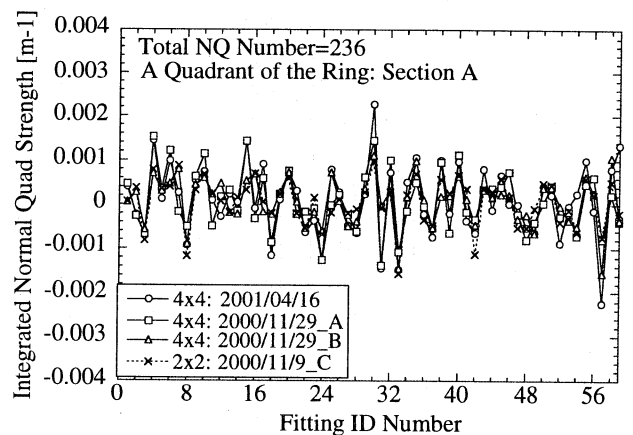


Figure 3: Integrated quadrupole error distributions.

As seen in Fig. 3 the estimated error distributions do not depend on the model used in MCM.

Figure 4 shows a quarter of the estimated skew quadrupole error distributions. In the figure, three distributions obtained by the different sets of beam responses are also shown. The slow harmonics of the distribution are well reproduced in every measurement. We see the magnitude of high harmonic components is less compared with that of the quadrupole error distribution.

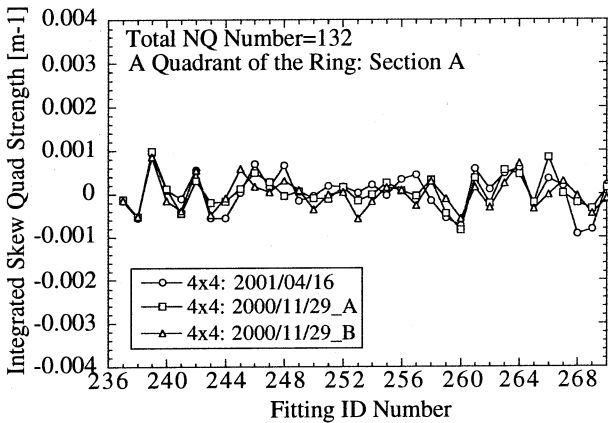


Figure 4: Integrated skew quadrupole error distributions.

3.4 Betatron Functions

Figure 5 shows estimated betatron functions for a quadrant of the ring. The betatron functions were calculated under the usual operation point ($\nu_x=40.15$, $\nu_y=18.36$), assuming the small shift of a operation point does not affect the error distribution seriously. In the figure, three kinds of distributions are shown together with the ideal distribution. One is estimated with the 2 by 2 formalism and others with the 4 by 4 one. In the 4 by 4 analysis, two different measurement data-sets were used. We see three kinds of distributions have a good agreement. The r.m.s. horizontal and vertical deviations are respectively $\sim 8\%$ and $\sim 6.5\%$.

The agreement between the results obtained with 2 by 2 and 4 by 4 formalisms shows the skew error fields are relatively weak. This means 2 by 2 formalism, where the off-diagonal parts of the one turn map are ignored, is good approximation for the SPring-8 storage ring.

3.5 Coupling Resonance Excitation

By using the estimated skew quadrupole fields, we can predict the excitation of linear coupling resonance lines around the operation point. The calculated excitation strength of the nearest resonance line, $\nu_x - \nu_y = 22$ agrees well with the value measured by the minimum tune separation. As seen in Fig. 6, we find one differential and two sum coupling resonance lines near by the operation point should be suppressed to achieve the small vertical emittance corresponding to the H-V coupling ratio of 0.1 %.

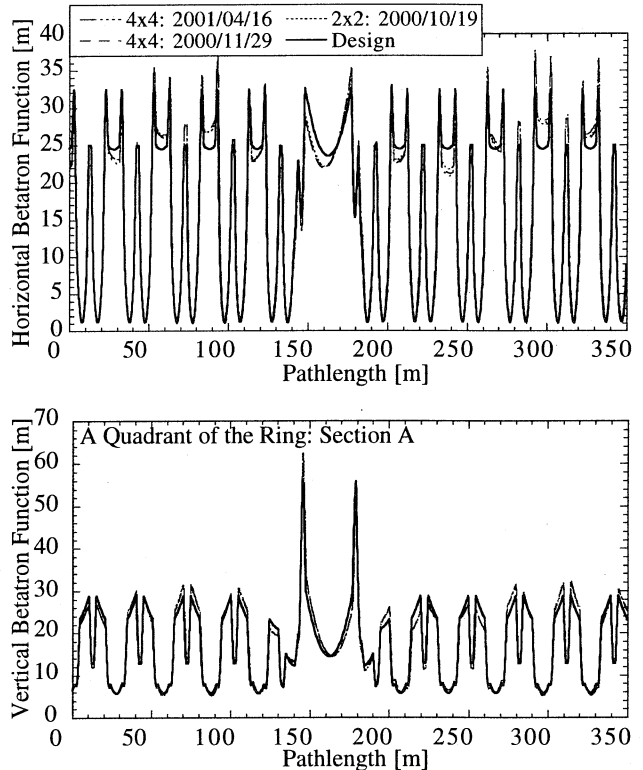


Figure 5: Distribution of betatron functions. Upper and lower graphs stand for respectively horizontal and vertical betatron functions.

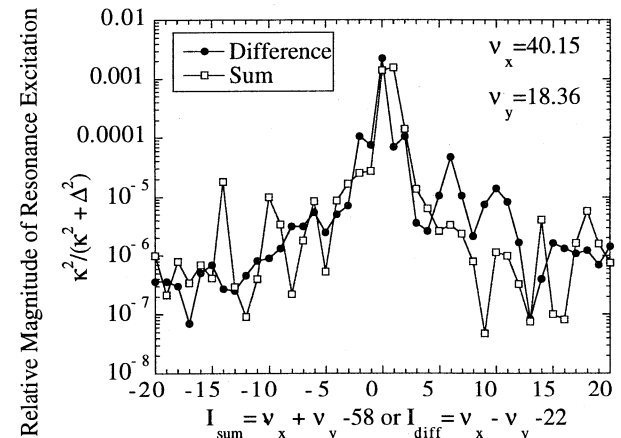


Figure 6: Excitation of linear coupling resonance near by the operation point.

4 REFERENCES

- [1] W.J. Corbett, M.J. Lee and V. Ziemann, SLAC-PUB-6111 (1993).
- [2] J. Safranek, N.I.M. A388 (1997) 27.
- [3] D. Robin, G. Portmann, H. Nishimura and J. Safranek, Proc. 5th EPAC, Barcelona, 10-14 June 1996, p.971.
- [4] G. Liu, K. Kumagai, N. Kumagai, H. Ohkuma, K. Soutome, M. Takao and H. Tanaka, Proc. 18th PAC, New York, 29 Mar.-2 Apr., 1999, p.2337.
- [5] H. Koiso, OHO'91, p.I-1-p.I-22 (1991) in Japanese, K. Ohmi, OHO'91, p.II-1-p.II-33 (1991) in Japanese.